

Microstructure and magnetic properties of graphite-coated Gd nanocapsules

X. G. Liu,^{a)} D. Y. Geng, Q. Zhang, J. J. Jiang, W. Liu, and Z. D. Zhang

Shenyang National Laboratory for Material Science, Institute of Metal Research, and International Centre for Material Physics, Chinese Academy of Sciences, 72 Wenhua Road, Shenyang 110016, People's Republic of China

(Received 21 January 2009; accepted 25 February 2009; published online 11 March 2009)

Gd nanocapsules, which are stable in air with the protection of graphite shells, are prepared by a modified arc-discharge technique. A size-induced structural transformation from the hexagonal-close-packed (hcp) to the higher-symmetry face-centered-cubic structure is observed. The graphite-coated hcp-Gd nanocapsules display a blocked state below 35 K, superparamagnetism between 35 and 290 K, and typical paramagnetism above 290 K. The hcp-Gd nanocapsules have a magnetic-entropy change $-\Delta S_m$ of $48.8 \text{ J kg}^{-1} \text{ K}^{-1}$ at 6 K for an applied-field change from 1 to 7 T. © 2009 American Institute of Physics. [DOI: 10.1063/1.3100618]

Magnetic refrigeration is a potentially highly energy-efficient cooling method, free of environmentally harmful working fluids. In contrast to the compression/expansion cycles characteristic of gas refrigerators, magnetic refrigeration relies on the magnetocaloric effect (MCE), the change in temperature associated with the magnetization/demagnetization of a magnetic refrigerant.¹⁻⁶ Recently, giant MCEs have been observed near room temperature at first- or second-order phase transitions. At lower temperatures ($T < 20 \text{ K}$), however, magnetic refrigeration can seldom be realized by employing these types of MCE because these phase transitions usually occur at higher temperatures. Based on the calculation of superparamagnetic theory, nanomagnets would have a larger magnetic-entropy change (ΔS_m) because of the existence of a large magnetic-moment density in a single magnetic particle.^{1,2,5} As a result, the research in MCE materials at lower temperatures is mainly focused on superparamagnetic nanocapsules. $\text{GdAl}_2/\text{Al}_2\text{O}_3$, $\text{TbAl}_2/\text{Al}_2\text{O}_3$, and $\text{HoAl}_2/\text{Al}_2\text{O}_3$ nanocapsules with large $-\Delta S_m$ at low temperatures have been prepared.^{2,4,6} However, the low thermal conductivity of the Al_2O_3 shell may decrease their application potential in a refrigeration process. Due to its metal-like thermal conductivity, graphite is a better candidate for the protective shell. Compared with transition-metals and their alloys, rare earths (REs) have a larger effective magnetic moment. However, RE atoms are very reactive in air which becomes a serious problem for nanoparticles with large surface areas. Hence, the preparation and characterization of nanostructured RE metals are a big challenge in nanoscience and nanotechnology. Here, we report on the synthesis, microstructure, magnetic properties, and cryogenic MCE of graphite-coated Gd nanocapsules prepared by a modified arc-discharge technique. This work may stimulate the preparation and investigation of the cryogenic MCE of other graphite-coated RE nanocapsules.

Compared with Ref. 7, some modified-strategies in the arc-discharge technique have been carried out for synthesizing the graphite-coated Gd nanocapsules. A 25 g Gd ingot of 99.9 wt % purity was used as the anode, while the cathode was a tungsten needle. The anode target was placed into a carbon crucible. Because Gd, as a potential candidate for

hydrogen-sensing and storage applications, easily absorbs hydrogen, possibly present hydrogen must be removed during the arc-discharge process.⁸ For the preparation of face-centered-cubic (fcc)-Gd nanocapsules, Ar (4 kPa) was introduced into a 0.004 Pa vacuum chamber. An arc with current of 20 A was generated between the anode and the cathode. For the production of hcp-Gd nanocapsules, more Ar (10 kPa) was introduced into the 0.004 Pa vacuum chamber. Then an arc with a larger current of 100 A was generated. It is a general fact that a larger amount of argon and a larger current are helpful for the formation of larger particles during the arc-discharge process. After the process of the arc discharge, the product was passivated in 10 kPa argon for 24 h. Phase-composition and microstructure analysis were performed by powder x-ray diffraction (XRD) with $\text{Cu } K\alpha$ radiation and high-resolution transmission electron microscopy (HRTEM) employing 300 kV. Magnetic measurements were carried out in a superconducting quantum interference device magnetometer.

Figure 1 shows the XRD patterns of fcc-Gd and hcp-Gd nanocapsules. In addition to several reflections indicating the existence of a small amount of GdC_2 , the main phase is fcc-Gd or hcp-Gd, depending on the amount of argon and the current in the arc-discharge process. It is worth noting that there are no detectable reflections of oxides, indicating that

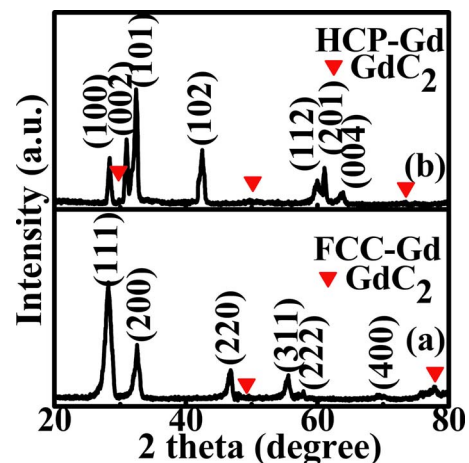


FIG. 1. (Color online) XRD patterns of (a) fcc-Gd and (b) hcp-Gd nanocapsules synthesized by arc-discharging bulk Gd.

^{a)}Electronic mail: liuxg@imr.ac.cn.

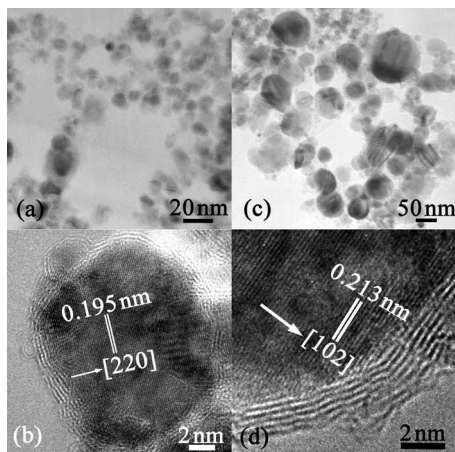


FIG. 2. (a) Morphology of fcc-Gd nanocapsules. (b) HRTEM image of an fcc-Gd nanocapsule. (c) Morphology of hcp-Gd nanocapsules. (d) HRTEM image of an hcp-Gd nanocapsule.

the two kinds of Gd nanocapsules are stable in air due to the protective shells. The average particle sizes of the fcc-Gd and hcp-Gd nanocapsules are 10.2 and 51 nm, respectively, as estimated by using the Scherrer equation. Upon decreasing particle size from 51 to 10.2 nm, the structure of the nanocapsules transforms from hcp to fcc. A single fcc phase has been reported for Gd nanoparticles of 8 nm capped by a Pd layer.⁹ So-called “bare” Gd nanoparticles with an average particle size of 7.0 nm have both hcp and fcc structure, and a single fcc phase was observed if the particle size is reduced to 5.0 nm.⁸ The present study shows that the structural transformation from fcc to hcp is solely an effect of the size. Size-induced structural transformations observed in other materials have been explained by increased ionic nature, modified surface structure, large concentration of defects present, or a change in the Gibbs free energy due to surface-energy contributions.^{10,11}

In Fig. 2(a), the morphology of fcc-Gd nanocapsules shows a spherelike shape and the average size is 10 nm, which is consistent with the XRD results in Fig. 1(a). A typical HRTEM image of a fcc-Gd nanocapsule, as shown in Fig. 2(b), clearly indicates that it has a “core/shell” type structure. In the core, the d -spacing of 0.195 nm corresponds to the lattice fringe {220} of fcc-Gd. The d -spacing in the coating layers is about 0.34 nm, corresponding to the {002} fringe of graphite. Figure 2(c) reveals the general morphology of hcp-Gd nanocapsules with a spherelike shape and an average size of 55 nm. In the outer shell, five layers of the {002} fringe of graphitic layers with 0.34 nm spacing are observed, and in the core, the d -spacing of 0.213 nm corresponds to the {102} fringe of hcp-Gd, as shown in Fig. 2(d). GdC₂ nanoparticles with smaller size were observed in the present sample (not shown here), which is different from the previous report on the graphite-coated CaC₂ nanocapsules.⁷ The formation of graphite-coated Gd nanocapsules and GdC₂ nanoparticles can be explained by the fact that C atoms from volatilization of the carbon crucible are easily absorbed by the Gd nanoparticles and subsequently condense to form a graphite layer on the surface. Some C atoms react with Gd nanoparticles with smaller size to form GdC₂ nanoparticles. However, the volatilization of the carbon crucible, due to the high temperature in the arc-discharge process, does not provide sufficient carbon atoms to react with Gd and to form

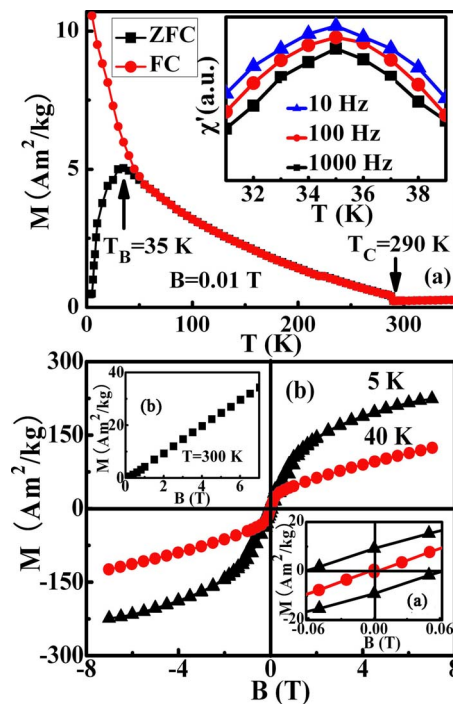


FIG. 3. (Color online) (a) ZFC and FC ($B=0.01$ T) magnetization curves of hcp-Gd nanocapsules. The inset shows the temperature dependence of the ac susceptibility at frequencies from 10 to 1000 Hz. (b) Magnetic hysteresis loops of hcp-Gd nanocapsules at 5 and 40 K, with the insets showing (a) the enlarged low-field part and (b) the magnetization curve at 300 K.

graphite shells on the surface of the GdC₂ nanoparticles.

It has been reported that fcc-Gd is paramagnetic and that the Curie temperature of hcp-Gd is 310 K.¹² The zero-field-cooled (ZFC) and field-cooled (FC) magnetization of the hcp-Gd nanocapsules, measured between 5 and 350 K in a magnetic field of 0.01 T, are shown in Fig. 3(a). From the maximum of the ZFC magnetization curve, the blocking temperature T_B of hcp-Gd nanocapsules, corresponding to a blocking process of the small particles, is determined to be 35 K. Below T_B , the sharp increase in the ZFC magnetization can be explained by the contribution of some small particles with T_B below 35 K. The temperature dependence of the ac susceptibility measured after ZFC [see inset of Fig. 3(a)] shows that the ac-susceptibility maximum remains unchanged as the frequency increases from 10 to 1000 Hz, which is different from the behavior of spin-glasses where the maximum shifts to lower temperatures.¹³ In addition, an anomaly in the two overlapping curves at 290 K corresponds to the Curie temperature T_C of hcp-Gd nanocapsules, which due to the size effect,⁴ is slightly lower than the 294 K for the bulk metal.¹⁴ The hysteresis loops at 5 and 40 K, obtained in ZFC measurements, show hysteretic behavior [Fig. 3(b)]. The coercive field at 5 K is 60 kA m⁻¹, indicating ferromagnetic behavior at low temperatures, but no coercivity is observed anymore at 40 K because the hcp-Gd nanocapsules are in the superparamagnetic state. Between T_B and T_C , the hcp-Gd nanocapsules show superparamagnetism because of their nanoscale size. At 300 K, the magnetization increases linearly with increasing magnetic field, showing typical paramagnetic behavior above T_C .

Generally, in case of materials in a blocked state, such as superparamagnetic particles, one cannot use the MCE resulting from a magnetic-field change to zero field where the

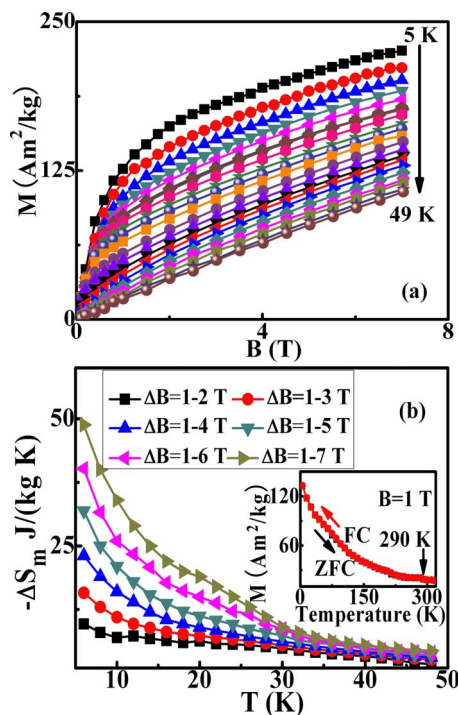


FIG. 4. (Color online) (a) Magnetic isotherms from 5 to 49 K in ZFC. (b) Temperature dependence of the magnetic-entropy change between 6 and 48 K for various applied-field changes. The inset presents ZFC and FC magnetization curves between 5 and 300 K, obtained in an applied field of 1 T.

entropy is not well defined due to the different zero-field magnetization values obtained in the FC and ZFC measurements. Also, in general, there is a drift in time of all the thermodynamic properties. Therefore, ΔS_m of the magnetic nanocapsules can better be defined between two states at finite magnetic-field values.¹ ΔS_m of the nanocapsules can be derived from magnetization data by using the Maxwell relationship given by $\Delta S_m(T, B) = \int_{B_1}^{B_2} (\partial M / \partial T)_B dB$. In the inset of Fig. 4(b), it is seen that the ZFC and FC curves exactly overlap in an applied field of 1 T, which indicates reversible magnetic behavior between 5 and 300 K. In Fig. 4(b), $-\Delta S_m$ of the hcp-Gd nanocapsules is shown between 6 and 48 K for various magnetic-field changes, obtained by means of the numerical approximation $\Delta S_m[(T_{n+1} + T_n)/2, B] = \sum [(M_{n+1} - M_n) / (T_{n+1} - T_n)] \Delta B$,¹ using the magnetic isotherms presented in Fig. 4(a), in which the increment in the temperature is 2 K from 5 to 49 K. The value of $-\Delta S_m$ increases with decreasing temperature for a certain applied-field change, and also increases with increasing applied-field change at a certain temperature. A $-\Delta S_m$ value of $9.7 \text{ J kg}^{-1} \text{ K}^{-1}$ is obtained at 6 K for a small field change from 1 to 2 T, while it reaches $48.8 \text{ J kg}^{-1} \text{ K}^{-1}$ upon a field change from 1 to 7 T.

Compared with $14.5 \text{ J kg}^{-1} \text{ K}^{-1}$ of $\text{GdAl}_2/\text{Al}_2\text{O}_3$ nanocapsules and $23.83 \text{ J kg}^{-1} \text{ K}^{-1}$ of $\text{TbAl}_2/\text{Al}_2\text{O}_3$ nanocapsules at 7.5 K in an applied-field change from 1 to 7 T,^{2,4} the $-\Delta S_m$ value of hcp-Gd nanocapsules reaches $42.3 \text{ J kg}^{-1} \text{ K}^{-1}$ upon a field change of 6 T at 7.5 K, which can be explained by the fact that the effective magnetic moment of Gd is larger than of GdAl_2 and TbAl_2 .

In summary, we have succeeded in preparing graphite-coated Gd nanocapsules, which are stable in air with the protection of graphite shells. The nanocapsules, with an average particle size of 51 nm, have the hexagonal structure. Upon reducing the particle size to 10.2 nm, a single fcc phase is observed. The values of T_B and T_C of graphite-coated hcp-Gd nanocapsules are 35 and 290 K, respectively. In a field change of 6 T, $-\Delta S_m$ quickly increases with decreasing temperature from 48 to 6 K and reaches $48.8 \text{ J kg}^{-1} \text{ K}^{-1}$ at 6 K. The present work shows that the modified arc-discharge technique can be utilized to prepare a family of nanocapsules of RE elements with the protective graphite shell. Graphite-coated hcp-Gd nanocapsules are very promising for magnetic refrigeration at temperatures around 6 K.

This work was supported by National Natural Science Foundation of China under Grant Nos. 50331030 and 50831006.

- ¹S. Ma, W. F. Li, D. Li, D. Y. Geng, and Z. D. Zhang, *Phys. Rev. B* **76**, 144404 (2007).
- ²S. Ma, D. Y. Geng, W. Liu, and Z. D. Zhang, *Nanotechnology* **17**, 5406 (2006).
- ³T. A. Yamamoto, M. Tanaka, and K. Niihara, *Jpn. J. Appl. Phys., Part 1* **39**, 4761 (2000).
- ⁴X. G. Liu, D. Y. Geng, J. Du, S. Ma, and Z. D. Zhang, *Scr. Mater.* **59**, 340 (2008).
- ⁵R. D. McMichael, R. D. Shull, and L. H. Bennett, *J. Magn. Magn. Mater.* **111**, 29 (1992).
- ⁶X. G. Liu, B. Li, D. Y. Geng, F. Yang, and Z. D. Zhang, *J. Phys. D* **42**, 045008 (2009).
- ⁷P. Z. Si, D. Y. Geng, X. G. Zhao, and Z. D. Zhang, *J. Appl. Phys.* **94**, 6779 (2003).
- ⁸X. G. Liu, J. J. Jiang, D. Y. Geng, and Z. D. Zhang, *Appl. Phys. Lett.* **94**, 053119 (2009).
- ⁹I. Aruna, B. R. Mehta, and S. M. Shivaprasad, *Adv. Mater. (Weinheim, Ger.)* **16**, 169 (2004).
- ¹⁰I. Aruna, B. R. Mehta, and S. M. Shivaprasad, *Adv. Funct. Mater.* **15**, 131 (2005).
- ¹¹J. N. Wickham, A. B. Herhold, and A. P. Alivisatos, *Phys. Rev. Lett.* **84**, 923 (2000).
- ¹²P. E. Chizhov, A. N. Kostigov, and V. I. Petinov, *Solid State Commun.* **42**, 323 (1982).
- ¹³Y. Sun, M. B. Salamon, and R. S. Averback, *Phys. Rev. Lett.* **91**, 167206 (2003).
- ¹⁴M. Yue, J. X. Zhang, H. Zeng, and K. J. Wang, *Appl. Phys. Lett.* **89**, 232504 (2006).